The structure of the turbulent pressure field in boundary-layer flows

By G. M. CORCOS

University of California, Berkeley

The paper is a discussion of measurements of the statistical properties of the pressure field at the wall of turbulent attached shear flows. These measurements have been made only in part by the author. A preliminary discussion is given of the important limitations imposed by the imperfect space resolution of contemporary pressure transducers. There follows a discussion of the appropriate scales of the pressure field. It is shown that measurements of the longitudinal cross-spectral densities lead to similarity variables for the space-time covariance of the pressure and for the corresponding spectra. The existence of these similarity variables may be due to the dispersion of the sources of pressure by the mean velocity gradient. Such a mechanism is illustrated by a simple model. Lateral cross-spectral densities also lead approximately to similarity variables.

Computations based directly upon detailed pressure-velocity correlation measurements by Wooldridge & Willmarth reveal that an important part of the pressure at the wall of a boundary layer is contributed by source terms which are quadratic in the turbulent velocity fluctuations; the interaction of the mean strain rate with normal velocity fluctuations, being in effect limited to a region very near the wall, supplies a dominant contribution only at high frequencies and its scales, downstream convective speed and convective memory are markedly smaller than those of the observed wall pressure.

The inner part of the Law of the Wall region ($y^* \leqslant 100$) seems to be substantially free of pressure sources and within that region (a) the pressure can be given in terms of its boundary value, and (b) the local velocity field is dependent upon but unable to affect appreciably the turbulent pressures.

Introduction

In an incompressible turbulent flow, the two dependent variables are velocity and pressure. Because such a flow is not irrotational, no kinematic solution is possible and because its dynamic equations are non-linear no simultaneous determination of pressure and velocity has been given no matter how simple the geometry of the flow or the boundary conditions. On the other hand, while a large number of measurements have permitted useful and informative experimental generalizations to be made, it seems fair to state that they have not supplied, to date, the physical basis for postulates which would be sufficient to initiate a theory of turbulence.

Largely because of the development of the hot-wire anemometer, experiments

had until recently favoured the measurement of instantaneous velocity fluctuations and the determination of statistical quantities derived from averages of these velocities. But a growing body of experimental literature is reporting measurements of pressure fluctuations. This is due in part to progress in measuring techniques, in part to an engineering interest in the pressure fluctuations themselves. For, whether pressure fluctuations solicit the motion of a flexible boundary (and thus cause the boundary to vibrate and to radiate a sound field) or couple directly with a surrounding fluid medium (generating aerodynamic noise) they are prime movers.

The following account is an attempt to interpret some of these pressure measurements. The discussion is not meant to be exhaustive and the reader will find treated elsewhere topics which have been omitted here. It must be admitted at the outset that the conclusions which are offered apparently provide only modest help to a theoretician although it is hoped that some of them will prove useful.

The experimental results which are the basis for the discussion are in part the author's own, in part due to a number of contributors, accounts of whose work are referenced in the text. However, the author gladly acknowledges the special value of one source of data: the excellent measurements made under W. Willmarth's guidance.

The defining equations

Consider an incompressible turbulent flow. The relevant Navier–Stokes equations provide us with a relation between fluctuating pressures and fluctuating velocities

$$\frac{\partial \mathbf{V}}{\partial t} + \mathbf{V} \cdot \operatorname{grad} \mathbf{V} + \frac{1}{\rho_0} \operatorname{grad} P = \nu_0 \operatorname{div} \operatorname{grad} \mathbf{V}, \tag{1}$$

where $\mathbf{V}$ is the velocity vector, ρ_0 and ν_0 are the density and the kinematic viscosity, both assumed constant, and P is the pressure. If we take the divergence of each term of this equation and make use of the continuity equation, i.e.

$$\operatorname{div} \mathbf{V} = 0$$

we obtain

$$\operatorname{div} \operatorname{grad} P = -\rho_0 \operatorname{div} \operatorname{div} (\mathbf{V}; \mathbf{V})$$

or in Cartesian index notation, wherein $\mathbf{V} = (V_i)$ and the position vector $\mathbf{x} = (x_i)$

$$\frac{\partial^2 P}{\partial x_i^2} = -\rho_0 \frac{\partial^2 V_i V_j}{\partial x_i \partial x_j}. \tag{2}$$

If we define, for a statistically stationary flow,

$$\mathbf{V}(\mathbf{x}, t) = \mathbf{U}(\mathbf{x}) + \mathbf{v}(\mathbf{x}, t),$$

where

$$\mathbf{U} = \lim_{T \to \infty} \frac{1}{T} \int_{t_0}^{t_0 + T} \mathbf{V} \, dt,$$

and likewise,

$$P(\mathbf{x}, t) = p_0(\mathbf{x}) + p(\mathbf{x}, t),$$

we may write, with $\mathbf{U} = (U_i)$,

$$\frac{\partial^2 p}{\partial x_i^2} = -X = -2\rho_0 \frac{\partial U_i}{\partial x_j} \frac{\partial v_j}{\partial x_i} - \rho_0 \frac{\partial^2}{\partial x_i \partial x_j} [v_i v_j - \overline{v_i v_j}], \tag{3}$$

in which an overbar denotes a time average similar to that used to define U.

The area scale of the pressure field

One of the very few inferences which can be made about the pressure on theoretical grounds alone concerns the instantaneous integral over a plane solid boundary of the pressure caused by an incompressible turbulent flow which is homogeneous in planes parallel to the boundary and which vanishes sufficiently fast in the direction normal to the boundary. This result may be applied to a two-dimensional boundary layer in the absence of an external pressure gradient, in so far as homogeneity along planes parallel to the boundary is well approximated over distances which are large when compared to a typical turbulence length scale. As Phillips has shown (1954), provided the velocity fluctuations vanish both at the boundary and at infinity (in a direction normal to the boundary), the momentum and continuity equations yield in this case

$$\left[\int \overline{p(\mathbf{x}, t)\, p(\mathbf{x} + \boldsymbol{\xi}, t)}\, dA(\boldsymbol{\xi}) \right]_{x_2 = 0,\, \xi_2 = 0} = 0, \tag{4}$$

where the normal distance from the boundary is x_2 or ξ_2 and the integration is carried over the whole plane of the boundary. Kraichnan (1956) gave an equivalent result in terms of the two-dimensional spectral function $E(0, k_1, k_3)$. Specifically, if

$$R(\xi_1, 0, \xi_3, 0) = \overline{p(x_1, 0, x_3, t)\, p(x_1 + \xi_1, 0, x_3 + \xi_3, t)},$$

and if one defines

$$E(0, k_1, k_3) = \frac{1}{4\pi^2} \int_{-\infty}^{\infty} \int_{-\infty}^{\infty} R(\xi_1, 0, \xi_3, 0) \exp \left\langle -i(k_1 \xi_1 + k_3 \xi_3) \right\rangle d\xi_1 d\xi_3,$$

then Kraichnan's result is that

$$\lim_{k_1, k_3 \to 0} E(0, k_1, k_3) = 0. \tag{5}$$

Hence the pressure correlation at the wall must be negative for some values of ξ_1 and ξ_3.

An approximate boundary condition

Equation (3) may be viewed as a Poisson equation for the fluctuating pressure p, in which case one imagines the right-hand side as a given scalar field. Boundary conditions are then required in terms of the pressure. At infinity we shall take $p = 0$. At the plane rigid wall of a turbulent boundary layer, Kraichnan (1956) examined the normal component of equation (1) in the light of velocity measurements in the vicinity of the sublayer and suggested that $(\partial p / \partial x_2)_{x_2 = 0} \cong 0$. A somewhat more detailed analysis by Lilley & Hodgson (1960) leads to the same result by showing that, at least in the absence of a mean pressure gradient, typical solutions of equation (3) are negligibly affected by such an approximation. Physically the demonstration consists in a comparison of a typical inertia term $\rho_0 v_j (\partial v_i / \partial x_j)$ with Townsend's (1956) estimate of $\left[\overline{(\partial p / \partial x_2)^2} \right]^{\frac{1}{2}}_{x_2 = 0}$ and so is equivalent to the boundary-layer approximations in steady flow. The two boundary conditions above permit the pressure at the wall to be given formally by

$$[p(\mathbf{x}, t)]_{x_2 = 0} = \frac{\rho_0}{2\pi} \int_{y_2 > 0} \frac{X(\mathbf{y}, t)}{|\mathbf{x} - \mathbf{y}|} d\sigma(\mathbf{y}), \tag{6}$$

where the integral is taken over the unbounded half-space above the boundary.

Measurement limitations

So far, all instantaneous pressure measurements in wall-attached shear flows have been made at the solid boundary. This is due in part to an intrinsic engineering interest in unsteady forces exerted on solid boundaries, in part to the fact that a probe introduced in the stream creates and records dynamic stresses which are different from the static pressure fluctuations. Thus our direct information is spatially limited.

There is another limitation which is perhaps worth mentioning at the outset because it seems to affect significantly almost all measurements of pressure fluctuations to date. This is the imperfect space resolution of the face of the pressure transducers used.

Transducer resolution

A transducer sensing element of non-zero size can only resolve adequately a spatial distribution of pressure, the length scale of which is greater than the characteristic dimensions of the transducer face. A similar problem arises in the use of hot-wire anemometry. The theoretical problem of the recovery of information at a point from the area average performed by the transducer may be viewed as the mapping of a random function of space by a linear operator. The mapping is a space integration and so some of the information is lost. The formalism is well understood (see, for instance, Uberoi & Kovasnay 1953), but it does not become useful until the lost information is supplied either by a postulate (say, isotropy) or by additional measurements. In the case of pressure transducers the problem has been analysed (Corcos 1963) with the help of the most detailed experimental information available to date about the space-time properties of the pressure field. A scheme was given to correct systematically experimental measurements of all statistical averages related to the space-time covariance of the pressure at least for a turbulent boundary layer. However, the correction is a very sensitive function of the apparent translation velocity of the pressure field about which our information is not yet of great accuracy.

When the correction is applied to available measurements, one finds that it is often prohibitively large. In fact, in most experiments the fine scale contribution to the pressure signal has been so attenuated by the probe as to have escaped detection, whereas extrapolation from the recorded frequency spectra for the smallest detected scale, properly corrected for transducer resolution, suggests that the contributions which have been overlooked may be an appreciable fraction of the signal. As a consequence, some important experimental quantities such as the fluctuating pressure intensity, and the apparent rate of downstream transport of the pressure field, may have been measured with important systematic errors which cannot yet be evaluated. Let us note that the correction factor for the pressure intensity is far from linear with transducer size so that extrapolations of pressure intensity from results obtained with inadequate transducer diameters are likely to be misleading.

The choice of non-dimensional parameters

It is well known that even when the Mach number, the degree of roughness and the longitudinal pressure gradient are eliminated as parameters, a turbulent boundary layer is not a self-similar flow in the sense that the average quantities are not functions of a single non-dimensional length or a single non-dimensional velocity. In the outer part of such flows, for instance, the mean velocity U_1 is referred both to the free-stream velocity U_∞ and to the so-called friction velocity
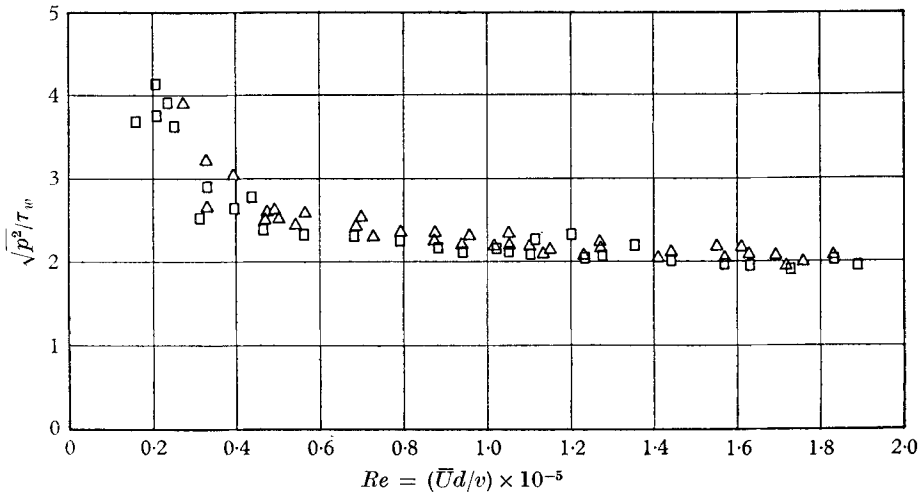
FIGURE 1. Turbulent pipe flow: the root-mean-square pressure at the wall as a function of Reynolds number. Correction for transducer size not applied but independent of Reynolds number.

$u^* = \sqrt{(\tau_w/\rho_0)}$ (where τ_w is the mean shear stress at the wall) and the dominant characteristic length is the boundary-layer thickness δ. In the inner part of the flow (the Law of the Wall region) the characteristic velocity is u^* and a length scale is taken as ν/u^*. But even in this limited region, and even if one considers only the coarse features of turbulence, this is not the only characteristic length. For instance, the frequency spectra of the downstream component v_1 of the velocity fluctuations are closely similar throughout the Law of the Wall region when plotted against $\omega\delta/U_1$ independently of the Reynolds number $u^*\delta/\nu$; whereas a non-dimensional frequency derived from the viscous length ν/u^*, i.e. $\omega\nu/U_1 u^*$, is grossly unable to bring into coincidence two v_1 spectra taken at the same non-dimensional distance, yu^*/ν, from the wall if the Reynolds number $u^*\delta/\nu$ is different.† Thus it is clear that at least some of the length scales found in the inner part of a boundary layer are impressed upon it by the characteristic length of the outer flow. The relationship between pressure and velocity fluctuations confers upon the pressure field scales which depend both on the scales of the velocity fluctuations and upon their distribution normal to the wall. Thus it is not obvious

† Such a comparison may be made from the data of Klebanoff (1954) and Wooldridge & Willmarth (1962) with a Reynolds number ratio of about 6 to 1.

a priori which parameters should be used in the presentation of pressure measurements. The evidence from existing data for boundary layers and pipe flows is relatively clear in this respect.
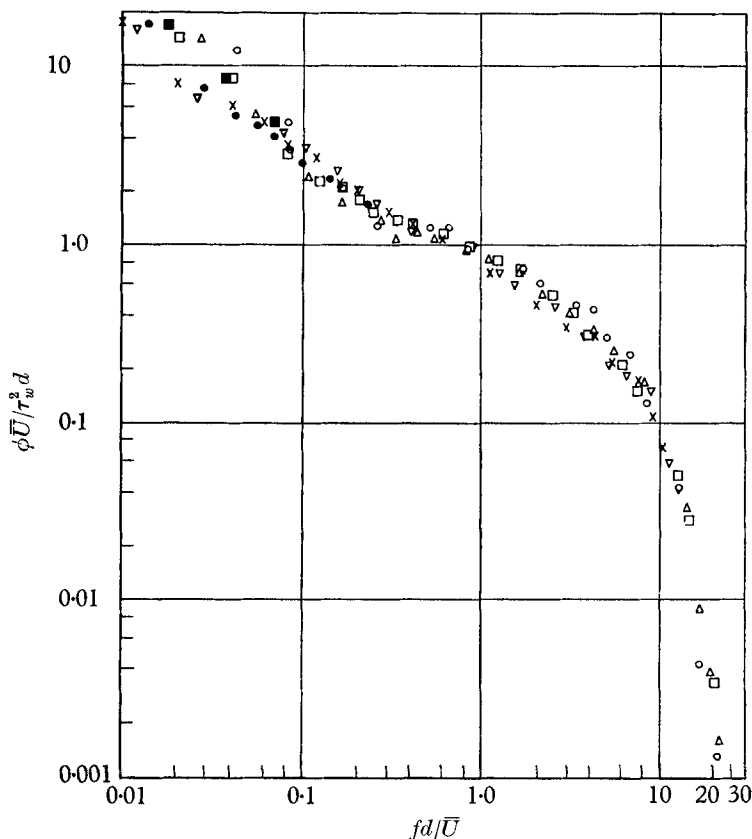

FIGURE 2. Frequency spectra of turbulent pressure at the wall (pipe flow). Correction for transducer size not applied but independent of Reynolds number.

$\bar{U}$, ft./s	$\sqrt{(\overline{p^2})}/\tau$	$Re \times 10^{-4}$	
○ 97	2·32	5·15	
△ 150	2·32	7·96	Piezo-electric element
□ 200	2·24	10·6	$(r = 0·02$ in.)
▽ 325	2·16	17·2	
× 410	2·09	21·8	
● 300	2·18	15·9	condenser mike
■ 150		7·96	

Variation with Reynolds number in the intensity $(\overline{p^2})$ of the wall-pressure fluctuations are minimized if the wall shear $\tau_w = \rho_0 u^{*2}$ is used to non-dimensionalize intensity. This is illustrated on figure 1 for fully developed turbulent pipe flow and confirmed by the measurements of Bakewell, Carey, Libuka, Schloemer & von Winkle (1962, pipe flow); of Hodgson (1962, subsonic boundary layers); and of Kistler & Chen (1962, supersonic boundary layer).

The length scale in the downstream direction (x_1) and lateral (x_3) directions

are clearly given by the over-all transversal extent of the shear flow—the pipe diameter d or the boundary-layer thickness δ. This is shown on figures 2 and 3. Figure 2 is a plot of the frequency spectral density of the pressure intensity for a pipe over a Reynolds number range of over four to one which was obtained by varying the pressure drop across the pipe. Figure 3 is borrowed from Bakewell
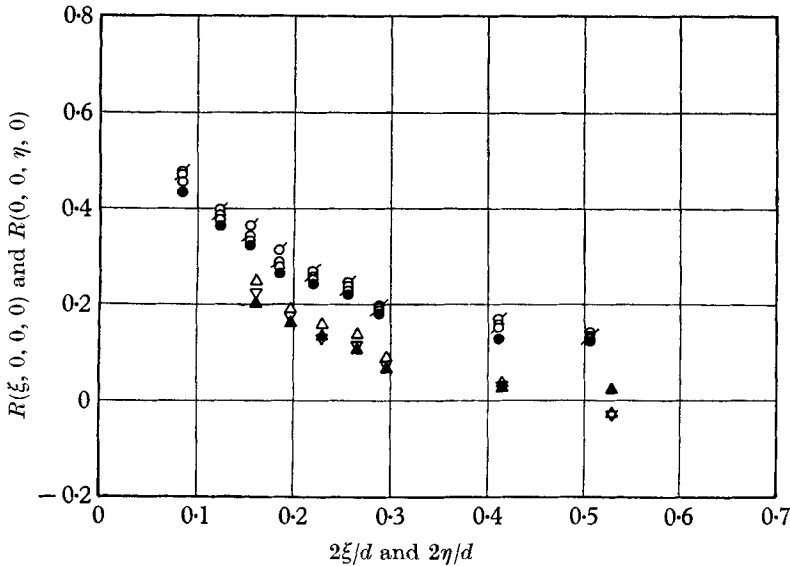

FIGURE 3. Space correlations of wall pressures in a pipe from Bakewell *et al.* (1962).

	$R_c = \bar{U}d/\nu$			$R_c = \bar{U}d/\nu$
Longitudinal correlation	◁	300,000	Lateral correlation	△ 300,000
	○	250,000		▽ 250,000
	○	200,000		▲ 150,000
	●	150,000		

et al. (1962) and shows lateral and longitudinal correlations of the pressure at the wall of a pipe to remain invariant over a friction length range of approximately two to one.

Thus as the thickness of the inner region of a turbulent boundary layer shrinks (higher free-stream velocity) the intensity of the pressure field remains approximately proportional to the intensity of the wall shear stress and the space scales of the pressure field at the wall remain approximately constant.

Intensity

The value of the pressure intensity, $\overline{p^2}$, has been measured by Harrison (1958), Willmarth (1957), Skudrzyk & Haddle (1960), Hodgson (1962), Willmarth & Wooldridge (1962), Bull (1963), and Serafini (1962) in subsonic two-dimensional flat plate boundary layers; von Winkle (1960), Corcos (1962), Bakewell *et al.* (1962) in fully developed turbulent pipe flow; and Bull & Willis (1961), Kistler & Chen (1962), and Richards (1961) in a supersonic boundary layer. In general resolution errors differed from one experiment to another and agreement even

after resolution errors have been allowed for is mediocre. A detailed analysis of all the subsonic boundary-layer data suggests only that perhaps at the wall $(p'/\tau_w) \cong 3.0 \pm 0.5$ for Reynolds numbers $U_\infty \delta/\nu \cong 300,000$ and that as has been remarked above the dependence of this ratio on Reynolds number appears to be small.† In turbulent pipe flows, the intensity is of the same order while in supersonic boundary layers the intensity seems to be larger—perhaps twice as large at a Mach number of 5·0.
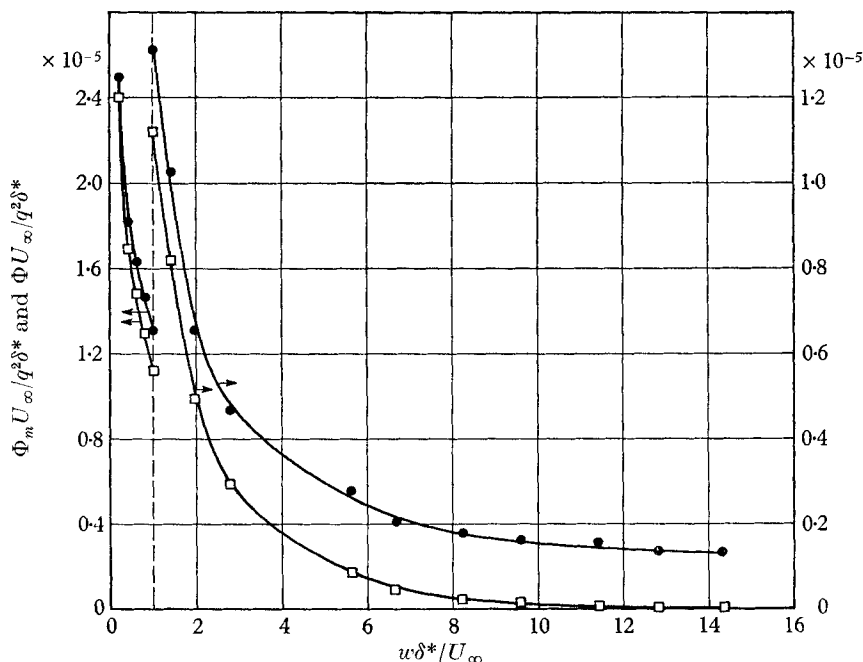

FIGURE 4. The frequency spectrum of wall pressure in a turbulent boundary layer. ●, Corrected for transducer resolution; □, Willmarth & Wooldridge (1962), uncorrrected.

Frequency spectra

The frequency spectral density of the pressure at the wall

$$\Phi(\omega) = \frac{1}{\pi} \int_0^\infty R(0,0,0,\tau) \cos \omega \tau \, d\tau$$

has also been measured by many. A large measure of disagreement is found among the reported values. Because the transducer resolution deteriorates as the frequency is increased, at high frequencies, the disagreement is primarily due to the difference in size and therefore in resolution of the transducers. Willmarth & Wooldridge (1962) achieved the best resolution to date† in a subsonic boundary layer with a ratio of transducer radius to boundary-layer thickness $r/\delta = 0.0193$. Their frequency spectrum is reproduced on linear scales on figure 4. Note the importance of the estimated size correction.

† See, however, Bull (1963).

At low frequencies important discrepancies may also be noted between the various measurements even under nominally equivalent conditions. Their origin is likely to be the presence of extraneous pressure contributions caused by secondary flows in the free stream, mass flow fluctuations and radiated noise. The spectra of Hodgson (1962), of Bull (1963) and of Serafini (1962) peak around $\omega\delta^*/U_\infty = 0\cdot2$; the spectral density then decreases to some extent with the frequency. This behaviour is accentuated in spectral measurements made on a glider by Hodgson (1962). In the glider measurements, the boundary layer at the measuring station was subjected to a moderately adverse pressure gradient.

Convective properties of the pressure field—similarity of the co-variances

It is known from the results of Favre, Gaviglio & Dumas (1957) that the spatial structure of the turbulent velocity field in a boundary layer is altered rather slowly if it is viewed in a preferred co-ordinate system which moves downstream with respect to stationary boundaries at a rate which depends on the distance from the wall at which the measurements are made: for a two-dimensional boundary layer we define, say,

$$\psi(x_2, \xi, \eta, 0, \tau) = \frac{\overline{v_1(x_1, x_2, x_3, t)\, v_1(x_1+\xi, x_2+\eta, x_3, t+\tau)}}{[\{v_1(x_1, x_2, x_3, t)\}^2 \{v_1(x_1+\xi, x_2+\eta, x_3, t+\tau)\}^2]^{\frac{1}{2}}}.$$

The function ψ peaks for pairs of values of ξ and τ (over a narrow range of values of η) which are such that $\xi/\tau = U_c$ is approximately constant and equal to the local mean velocity U_1 (figure 5). This velocity will be called a convection velocity. For a judicious choice of (small) η the peaks decrease slowly as the downstream separation ξ increases. In the outer part of the boundary layer the optimum space-time correlation exceeds $0\cdot5$ for separation distances equal to many boundary-layer thicknesses. For the inner part of the layer this convective auto-correlation is shorter-lived: for $y/\delta = 0\cdot06$ it drops to a value of $0\cdot5$ over the time required for a downstream travel equal to about one boundary layer thickness.

Early measurements by Willmarth (1957) revealed that the pressure field at the wall reflected this behaviour. Longitudinal space-time measurements of the fluctuating pressure at the wall of a boundary layer yielded correlations which peaked for pairs of values of τ and ξ such that $(\xi/\tau U_\infty) = 0\cdot82$. More recently, many authors have obtained similar results in turbulent boundary layers and pipe flows. Willmarth & Wooldridge (1962) gave a particularly detailed mapping of the longitudinal space-time correlation which indicated a progressive increase in the convection velocity U_c as the distance between the two measuring stations was increased. The apparent convection of the pressure field at the boundary is clearly due to the combined translation of the sources of pressure within the turbulent flow.

We may profitably view the space-time correlations of the pressure as a Fourier synthesis with respect to time of individual frequency components.

For a point on the boundary let us define a cross-spectral density $\Gamma(\xi, \eta, \omega)$ by

$$R(\xi, \eta, \tau) = \int_{-\infty}^{+\infty} \exp\left(i\omega\tau\right) \Gamma(\xi, \eta, \omega)\, d\omega. \tag{7}$$

where $R(\xi, \eta, \tau) = \overline{p(x_1, 0; x_3, t)\, p(x_1 + \xi, 0, x_3 + \eta, t + \tau)}$. Since $R(\xi, \eta, \tau)$ is real, the real part of Γ is symmetric and the imaginary part anti-symmetric in ω and

$$R(\xi, \eta, \tau) = \int_0^\infty |\Gamma| \cos(\omega\tau + \alpha)\, d\omega.$$

If the output of two pressure transducers $(\xi, 0)$ apart is filtered by two identical and (infinitely) narrow band-pass filters of, say, unit width, the mean of the product of their output is a non-decaying periodic function of τ

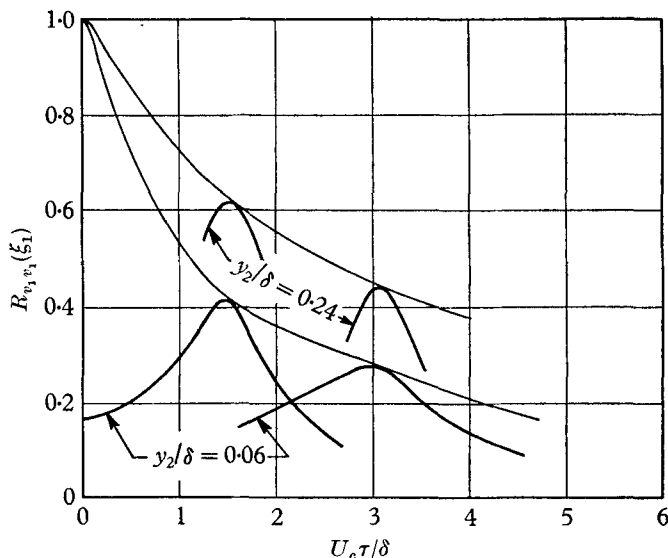$$R_\omega(\xi, 0, \tau) = |\Gamma(\xi, 0, \omega)| \cos(\omega\tau + \alpha).$$

FIGURE 5. The space-time correlation of longitudinal velocity fluctuations from Favre *et al.* (1957).

$|\Gamma|$, the amplitude of this periodic function and α its phase angle are readily measured. This was done by Corcos (1962), Willmarth & Wooldridge (1962), and Bakewell *et al.* (1962). It is clear that in principle such measurements are equivalent to the direct recording of space-time correlation. But they possess over the latter at least two advantages. They allow (Corcos 1963) a systematic correction for transducer size. Also, they exhibit explicitly what we shall call the similarity properties of the covariance of the pressure field.

These properties are derived from the result that the complex function Γ, when rendered non-dimensional, is nearly a function of a single similarity variable which involves ω and ξ as a product. Specifically: if the angle α is used to define an average translation velocity $U_c(\omega, \xi)$ by

$$\alpha = -\omega\xi/U_c, \tag{8}$$

then the ratio A defined by

$$A = |\Gamma(\omega, \xi)|/\Phi(\omega) \tag{9}$$

is found to be approximately a function of $\omega\xi/U_c$ only, while U_c/U_∞ is found to be a weak function both of $\omega\delta^*/U_\infty$ and of ξ/δ^*. The similarity variable upon which both the magnitude and the argument of Γ depend is therefore $\omega\xi/U_c$. The magni-

tude $|\Gamma|$ is a measure of the convective memory of a frequency component and its dependence on $\omega\xi/U_c$ only implies that this memory is approximately independent of the characteristic frequency of the flow, say, U_∞/δ^*. The evidence in
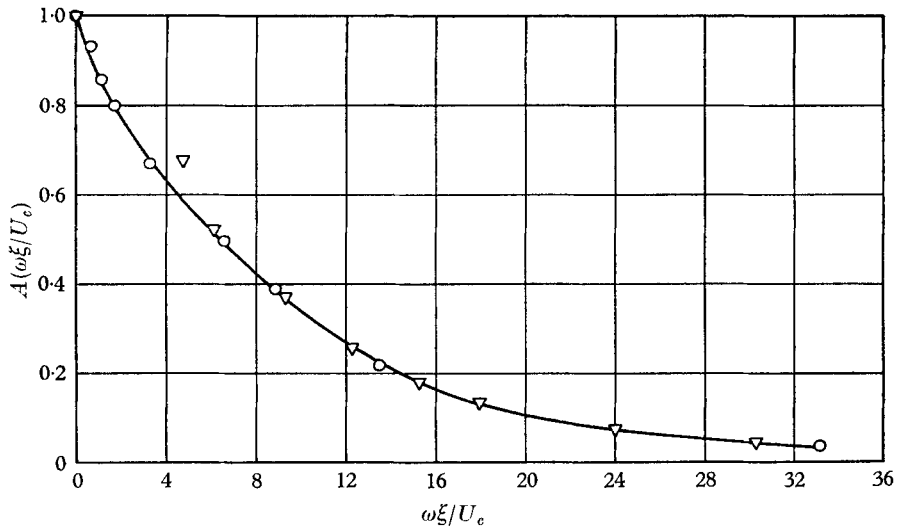

FIGURE 6. The amplitude of the cross-spectral density in a boundary layer, from Willmarth & Wooldridge (1962). $\triangledown$, $\omega\delta^*/U_\infty = 5\cdot00$; $\bigcirc$, $\omega\delta^*/U_\infty = 0\cdot68$.
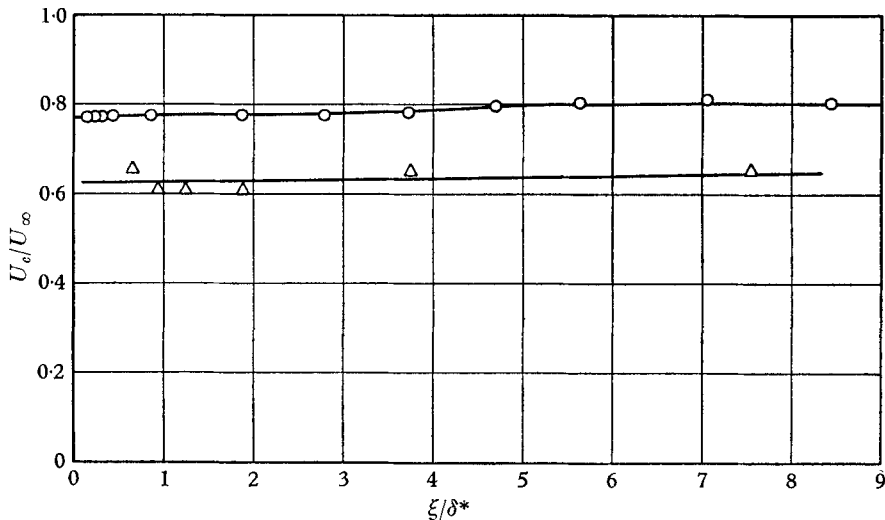

FIGURE 7. The convection velocity in a boundary layer. Data from Willmarth & Wooldridge (1962). $\triangle$, $\omega\delta^*/U_\infty = 5\cdot00$; $\bigcirc$, $\omega\delta^*/U_\infty = 0\cdot68$.

favour of this result is provided by the measurements of Willmarth & Wooldridge (1962) and by us, and is somewhat more weakly brought out by Bull (1963), Bakewell *et al.* (1962), Hodgson (1962), and Harrison (1958),[†] who first made cross-spectral density measurements.

[†] The data as presented by the three authors mentioned last appears to require large systematic corrections due to the finite band width of the filters used (cf. Corcos 1962, appendix).

In a turbulent boundary layer, Willmarth & Wooldridge measured both A and α for a range of separations of ξ and for two widely separated frequency bands centred around $\omega\delta^*/U_\infty = 0{\cdot}68$ and $\omega\delta^*/U_\infty = 5{\cdot}45$. Their data† is presented on figure 6 where A is plotted as a function of $\omega\xi/U_c = -\alpha$ with $\omega\delta^*/U_\infty$
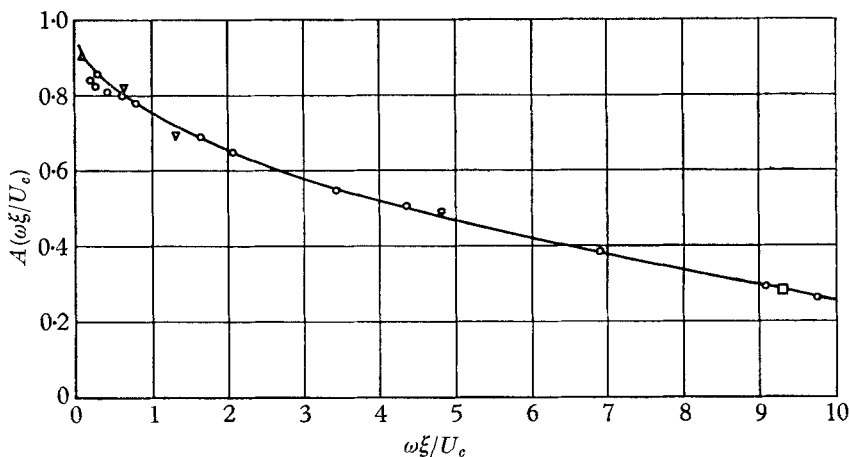

FIGURE 8. The amplitude of the cross-spectral density in a pipe. ξ/d: $\bigcirc$, $0{\cdot}2$; $\triangle$, $0{\cdot}15$; $\triangledown$, $0{\cdot}75$; $\square$, $11{\cdot}2$.
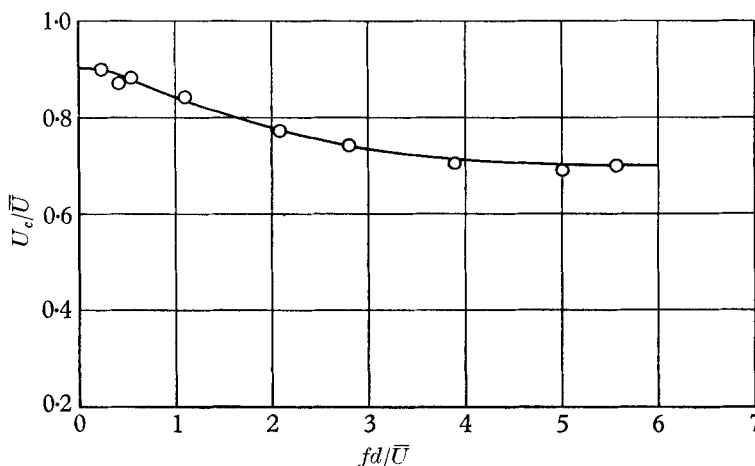

FIGURE 9. The convection speed as a function of frequency in a pipe.

as a parameter and on figure 7 where U_c/U_∞ is plotted as a function of ξ/δ^* with $\omega\delta^*/U_\infty$ as a parameter. Note that U_c/U_∞ varies relatively little with ξ/δ^* and more with $\omega\delta^*/U_\infty$.

Similar measurements were obtained in pipe flow with fewer separation

† The values presented here are not those quoted by the authors. Our definition of translation velocity (equation (8)) differs from the one they used. Also, since the band-pass was wide, the effective frequency of the filter was different from the centre frequency whenever the spectral density varied appreciably within the band-pass. This happened for the higher frequency band.

distances and a greater number of frequency bands. The corresponding plots of A and $U_c/\bar{U}$ (where $\bar{U}$ is the mean discharge velocity for the pipe) are given in figures 8 and 9.

We shall see that the accuracy to which Γ depends only on $\omega\xi/U_c$ can be checked in detail from independent measurements of Willmarth & Wooldridge.

Longitudinal space-time correlations and two-dimensional spectra

As might be expected, the fact that the amplitude function A is approximately a function of the phase angle α only has strong consequences for the correlation $R(\xi, \tau)$ and the related spectral function $E_1(k_1, \omega)$. For our wall pressure field assumed stationary and x-wise homogeneous, we define the full Fourier transform

$$E_1(k_1, \omega) = \frac{1}{4\pi^2} \int_{-\infty}^{\infty} \int_{-\infty}^{\infty} R(\xi, \tau) \exp \langle -i(k_1\xi + \omega\tau) \rangle \, d\xi \, d\tau, \tag{10}$$
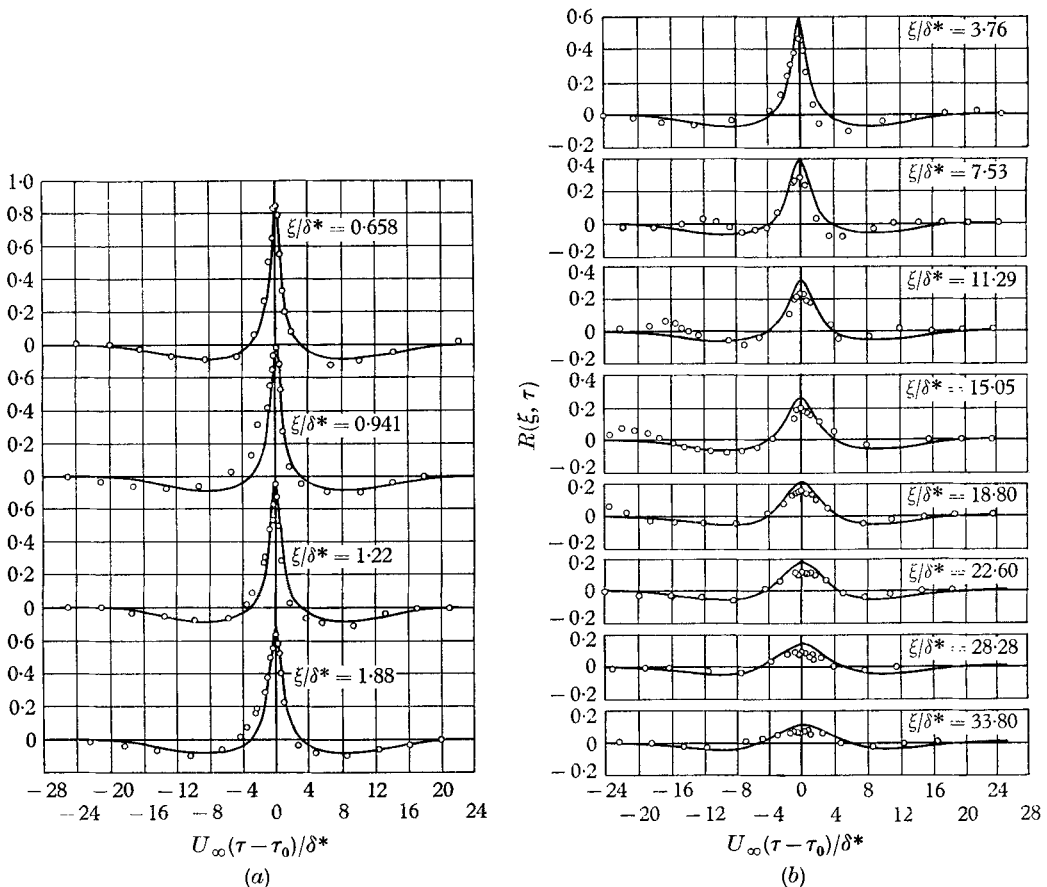

FIGURE 10. A check of the similarity variable $\omega\zeta/U_c$.

$$R(\xi, \tau) = \frac{1}{\overline{p^2}} \int \Phi(\omega) \, A\,(\omega\xi/U_c) \cos\omega(\tau - \xi/U_c) \, d\omega.$$

○, Experimental points Willmarth & Wooldridge (1962).

and from equation (7)

$$\Gamma(\xi,\omega) = \frac{1}{2\pi} \int_{-\infty}^{\infty} \exp\left(-i\omega\tau\right) R(\xi,\tau)\, d\tau = \int_{-\infty}^{\infty} \exp\left(ik_1\xi\right) E_1(k_1,\omega)\, dk_1. \quad (11)$$

Then, in view of the experimental results discussed above, we can write approximately

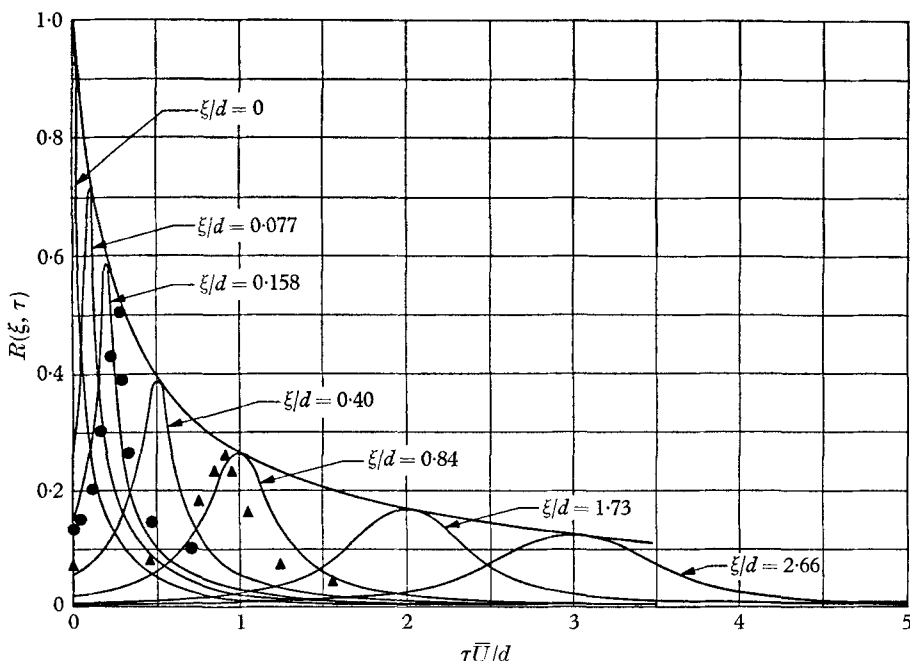$$\Gamma(\xi,\omega) = \Phi(\omega)\, A(\omega\xi/U_c) \cos(\omega\xi/U_c), \quad (12)$$

FIGURE 11. Longitudinal space-time correlations in a pipe. Solid lines are Fourier transforms of cross-spectral density. ▲, Direct measurement $\xi/d = 0\cdot2$ in; ●, direct measurement $\xi/d = 0\cdot75$ in.

from which it follows, E_1 being real, that

$$E_1(k_1,\omega) = \frac{1}{\pi} \int_0^{\infty} \Gamma(\xi,\omega) \cos k_1\xi\, d\xi = \frac{U_c\Phi(\omega)}{\pi|\omega|} \int_0^{\infty} A\left(\frac{\omega\xi}{U_c}\right) \cos\left\{\frac{k_1 U_c}{\omega}\left(\frac{\omega\xi}{U_c}+1\right) d\left(\frac{\omega\xi}{U_c}\right)\right\},$$

or

$$E_1(k_1,\omega) = \frac{U_c\Phi(\omega)}{|\omega|} E_0(\mu+1), \quad (13)$$

where $\mu = k_1 U_c/\omega$ and E_0 is the cosine Fourier transform of A,

$$E_0(\nu) = \frac{1}{\pi} \int_0^{\infty} A(\beta) \cos\nu\beta\, d\beta.$$

In the integration leading to equation (13), $k_1 U_c/\omega$ is required to be fixed so that U_c must be independent of ξ for a given ω. Figure 7 suggests that this condition is closely satisfied. On the other hand, according to equations (7) and (12)

$$R(\xi,\tau) = \int_0^{\infty} \Phi(\omega)\, A(\omega\xi/U_c) \cos(\omega\tau - \xi/U_c)\, d\omega. \quad (14)$$

A direct check on the accuracy with which similarity variables yield space-time correlations from the frequency spectrum $\Phi(\omega)$ and the amplitude of the function $A(\omega\xi/U_c)$ is presented in figures 10 and 11 where predictions obtained from a numerical integration of the integrand in equation (14) are compared with direct measurement of the space-time correlation in a boundary layer (Willmarth & Wooldridge 1962) and in a pipe. The agreement, particularly in the case of the boundary layer, seems convincing.

Similarity and Taylor's hypothesis

Taylor's hypothesis suggested that for low turbulence levels and uniform mean flow (turbulence behind grids) apparent changes in time at a fixed station are almost entirely due to the translation of spatial non-uniformity past a fixed observer, i.e.
$$v_i(x_1, t) \simeq v_i(x_1 - U_c t, 0),$$
or in terms of correlations
$$R_{ii}(0, \tau) = \overline{v_i(x_1, t) \, v_i(x_1, t+\tau)} = \overline{v_i(x_1, t) \, v_i(x_1 - U_c \tau, t)} = R_{ii}(-U_c \tau, 0),$$
which can be written
$$R_{ii}(\xi, 0) = \int_0^\infty \Phi_{ii}(\omega) \cos(\omega\xi/U_c) \, d\omega. \tag{15}$$

The difference between equations (14) and (15) for space correlations with no time delay (where R_{ii} and Φ_{ii} are replaced by the corresponding pressure correlations and pressure spectral densities) is numerically quite small because for all combined values of ξ and ω for which neither $R(\xi)$ nor $\Phi(\omega)$ are negligible, $A(\omega\xi/U_c)$ is relatively close to unity. However, the fact that U_c is a decreasing function of frequency implies that for small separation distances ξ, $R(\xi, 0)$ falls more rapidly and for large ξ less rapidly according to equation (14) than would be the case if an average translation velocity were assumed (as is usually done in applications of Taylor's hypothesis). This is illustrated on figure 12 where equations (15) (with a fixed U_c) and (14) have been applied to our pipe data.

It will be shown later that the assumption of a locally frozen velocity field obeying Taylor's hypothesis leads to space-time correlations for the pressure at the wall which are essentially similar in the sense defined above.

The integral time scale of the pressure at the wall

It is apparent from figures 10 and 11 that, according to the similarity hypothesis, the correlation curves widen as their amplitude decreases. In fact the integral scale
$$T_\xi = \int_0^\infty R(\xi, \tau)/R(0, 0) \, d\tau$$
is independent of ξ. By definition
$$\Gamma(0, \omega) = \frac{1}{\pi} \int_0^\infty \cos \omega\tau \, R(0, \tau) \, d\tau = \Phi(\omega),$$
so that the function $A(\omega, \xi) = \{\Gamma(\omega, \xi)/\Phi(\omega)\} \cos(\omega\xi/U_c)$ tends to unity as $\xi \to 0$ whether A is truly a function of $\omega\xi/U_c$ or not. On the other hand
$$\Gamma(\xi, 0) = (2\pi)^{-1} \int_{-\infty}^\infty R(\xi, \tau) \, d\tau = (2\pi)^{-1} R(0, 0) \, T_\xi.$$

But according to the similarity hypothesis, and defining $T_0 = T_\xi$ for $\xi = 0$,

$$\Gamma(0, \xi) = \Phi(0) = (2\pi)^{-1} R(0, 0) T_0; \tag{16}$$

i.e. $T_0 = T_\xi = \text{const.}$ The assumption used for this result, namely that A depends only on $\omega\xi/U_c$ no matter how small this variable, is not supported by strong experimental evidence (figures 6 and 8) but the space-time correlations measured in turbulent boundary layers and pipes come quite close to satisfying equation (16).
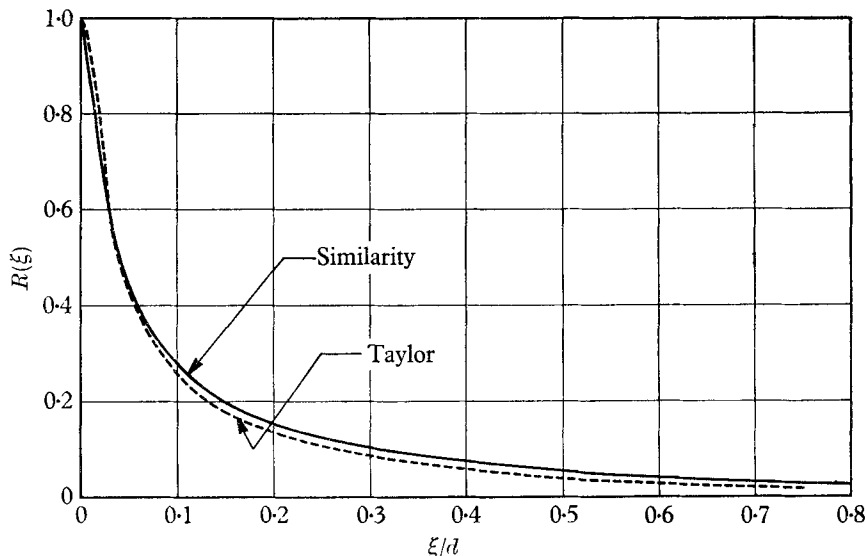

FIGURE 12. The longitudinal correlation in a pipe. Taylor's hypothesis

$$R(\xi) = \frac{1}{p^2} \int_0^\infty \Phi(\omega) \cos \frac{\omega\xi}{U_c} \, d\omega;$$

and the similarity hypothesis

$$R(\xi) = \frac{1}{p^2} \int_0^\infty \Phi(\omega) A\left(\frac{\omega\xi}{U_c}\right) \cos \frac{\omega\xi}{U_c} \, d\omega.$$

It thus seems that as a given pressure pattern is translated downstream it does not become incoherent so much as spread out. In fact it is possible to account for these features of the longitudinal space-time correlation as the result of the dispersive effect of the mean velocity gradient on the pressure sources on the assumption that the pressure field is contributed by a number of sources which are translated over a range of velocities $U_c(x_2)$ and which retain convective-auto-correlation for a long time. It can be seen from a simple example that departures from similarity may be a measure of the relative importance of the convective lack of coherence of a given source and of the dispersive action of the mean velocity gradient upon the contributing sources.

Without identifying the sources specifically, we write, according to equation (6) for a point at the boundary with co-ordinates $(0, 0, 0)$

$$p(0, 0, 0, t) = \frac{\rho_0}{2\pi} \int_{y_2 > 0} \frac{X(\mathbf{y}, t)}{|\mathbf{y}|} \, d\sigma(\mathbf{y}).$$

Likewise for another point on the wall, a distance ξ downstream of the first,

$$p(\xi, 0, 0, t+\tau) = \frac{\rho_0}{2\pi} \int_{y_2' > 0} \frac{X(\mathbf{y}', t+\tau)}{|\mathbf{y}' - \mathbf{i}\xi|} d\sigma(\mathbf{y}'),$$

where $\mathbf{i}$ is the unit vector in the downstream direction. Hence the correlation between pressure at the two points is

$$R(\xi, \tau) = \frac{\rho_0^2}{4\pi^2} \int_{y_2 > 0} \int_{y_2' > 0} \frac{\overline{X(\mathbf{y}, t) \, X(\mathbf{y}', t+\tau)} \, d\sigma(\mathbf{y}) \, d\sigma(\mathbf{y}')}{|\mathbf{y}| \, |\mathbf{y}' - i\xi|}.$$

Call $\mathbf{y}' - \mathbf{y} = \mathbf{x}$ and assume that the correlation $\overline{XX'}$ is that between infinitesimally spread sources convected at speeds $U_c(y_2)$ and perfectly correlated in time in a convective frame of reference, so that

$$\overline{X(\mathbf{y}, t) \, X(\mathbf{y}', t+\tau)} = \overline{M'^2}(y_2) \, \delta(x_1 - U_c \tau) \, \delta(x_2) \, \delta(x_3) \, \lambda_1 \lambda_2 \lambda_3;$$

$\overline{M'^2}$ is the intensity of the source at y_2, $\lambda_{1,2,3}$ are three lengths scales of the source, $\delta(\nu)$ is a Dirac delta function and U_c is a function of y_2.

Then substituting and integrating with respect to $\mathbf{x}$, we have

$$R(\xi, \tau) = \frac{\rho_0^2 \lambda_1 \lambda_3}{4\pi^2} \int_{y_2 > 0} \frac{\overline{M'^2} \lambda_2 \, d\sigma(\mathbf{y})}{|\mathbf{y}| \, |\mathbf{y} + \mathbf{i}U_c\tau - \mathbf{i}\xi|}. \tag{17}$$

Thus, $R(\xi, \tau)$ has the following properties. For $\tau = 0$, the correlation decreases as ξ increases. For $\xi = 0$, the correlation decreases as τ increases.

Since U_c is a function of y_2, the effective value of $|\mathbf{y} + \mathbf{i}U_c\tau - \mathbf{i}\xi|$ is always greater than $|\mathbf{y}|$ over the integral for $\xi \neq 0$ so that even at an optimum τ, the correlation decreases as ξ increases.

Finally, the time scale

$$\frac{1}{R(0, 0)} \int_{-\infty}^{\infty} R(\xi, \tau) \, d\tau$$

can be rewritten for any single y_2 with $\tau' = \tau - (\xi/U_c)$ and integrated with respect to τ first. The time scale then becomes invariant with respect to ξ,

$$\int_{-\infty}^{\infty} R(\xi, \tau) \, d\tau = \int_{-\infty}^{\infty} R(0, \tau) \, d\tau = \text{const.}$$

The very simple model above has the properties which we have approximately attributed to the real pressure field. Thus the dispersion of the sources of pressure by the mean stream may well be the dominant mechanism responsible for the convective lack of coherence of the pressure (departure from Taylor's hypothesis). But the model also warns us that inferences cannot be made about the detailed structure of the velocity or of the vorticity field from measurements of the pressure at the wall because the pressure is rather insensitive to these details.

Lateral correlation—generalized similarity variables

For a boundary layer, Willmarth & Wooldridge (1962) and, for a pipe, Bakewell *et al.* (1962) have measured the cross-spectral density of the lateral correlation, i.e. the function $\Gamma(0, \eta, \omega)/\Phi(\omega)$. In both cases the data suggest that the filtered

G. M. Corcos

correlation amplitudes have a lateral scale which is nearly proportional to $1/\omega$. One may define

$$\Gamma(0, \eta, \omega) = \frac{1}{2\pi} \int_{-\infty}^{\infty} R(\eta, \tau) \exp\left(-i\omega\tau\right) d\tau,$$

so that
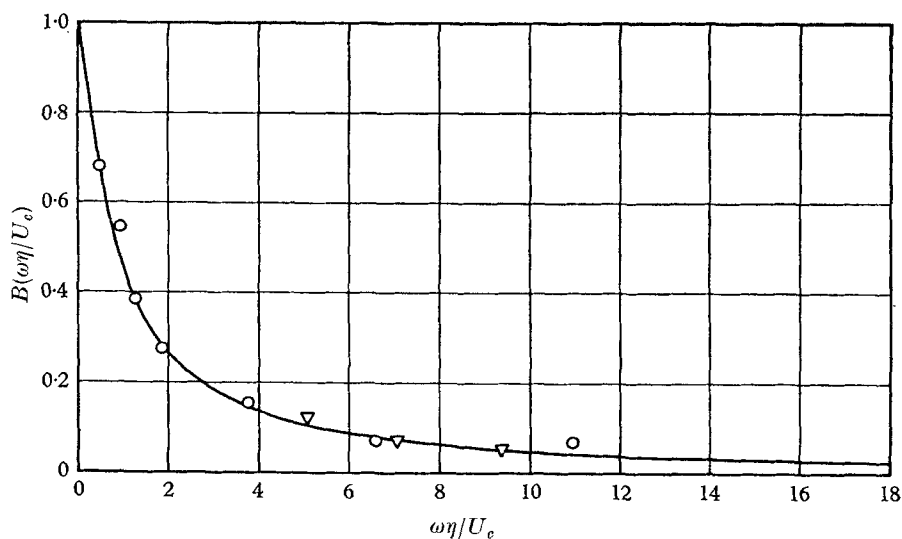$$R(0, \eta, 0) = 2 \int_{0}^{\infty} \Gamma(0, \eta, \omega) \, d\omega. \tag{18}$$

FIGURE 13. The lateral cross-spectral density in a boundary layer from Willmarth & Wooldridge (1962). $\bigcirc$, $\omega\delta^*/U_\infty = 0.68$; $\triangledown$, $\omega\delta^*/U_\infty = 5.00$.
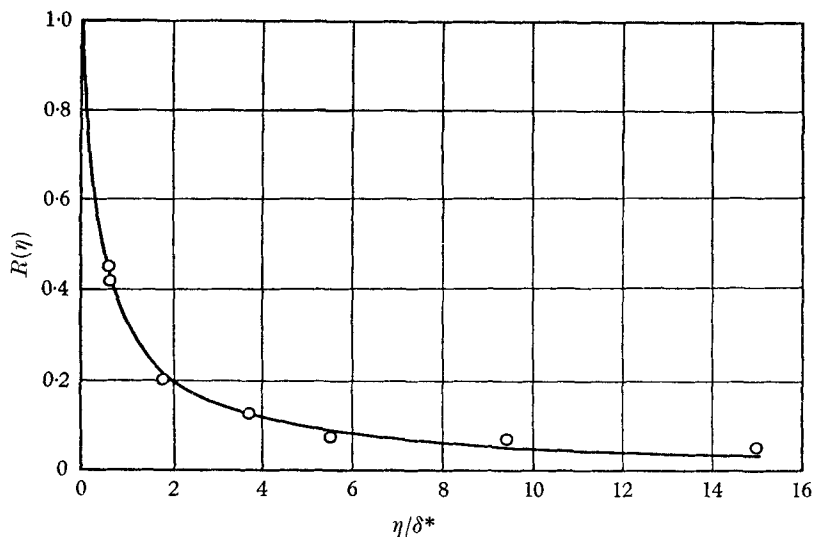

FIGURE 14. Lateral correlation; test of the similarity variable $\omega\eta/U_c$. $\bigcirc$, Measured (Willmarth & Wooldridge); ——, computed from $R(\eta) = \int \Phi(\omega) \, B\left(\frac{\omega\eta}{U_c}\right) d\omega$.

The data presented on figure 13 indicates that approximately

$$\Gamma(0, \eta, \omega) = \Phi(\omega) \, B(\omega\eta/U_c)$$

so that

$$R(0, \eta, 0) = \int_{-\infty}^{\infty} \Phi(\omega) \, B\left(\frac{\omega n}{U_c}\right) d\omega. \qquad (18a)$$

If for Willmarth's boundary layer, one computes $R(0, \eta, 0)$ from $(18a)$ by using measured values of $\Phi(\omega)$ and of $B(\omega\eta/U_c)$ one obtains (figure 14) a lateral correlation in excellent agreement with measured values.

The location and nature of the pressure sources

The experimental results which have been discussed and formal solutions such as equation (6) lead us to expect that the spatial structure of the turbulent pressure in a shear flow is not as fine-grained as that of the velocity field and one may well wonder whether the pressure is not defined more simply than a literal reading of equation (3) would suggest.

The motivation for simplifying equation (3) is very strong. For instance, it can be seen from equations (3) and (6) that a quantity as simple as $(\overline{p^2})_{x_2=0}$ is given by

$$[\overline{p^2}(\mathbf{x})]_{x_2=0} = \frac{\rho_0^2}{4\pi^2} \int_{y_2'>0} \int_{y_2''>0} \frac{\overline{X(\mathbf{y}',t) \, X(\mathbf{y}'',t)}}{|\mathbf{x}-\mathbf{y}'| \, |\mathbf{x}-\mathbf{y}''|} \, d\sigma(y') \, d\sigma(y''), \qquad (19)$$

where $d\sigma$ is an element of volume, the integration is twofold over the space $y_2' > 0$ and $y_2'' > 0$ and where

$$\overline{X(\mathbf{y}') \, X(\mathbf{y}'')} = 4 \frac{\partial U_i}{\partial y_j'} \frac{\partial U_k}{\partial y_l''} \overline{\frac{\partial v_j \partial v_l}{\partial y_i' \partial y_k''}} + 4 \frac{\partial U_i}{\partial y_j'} \overline{\frac{\partial v_j}{\partial y_i'} \frac{\partial v_k}{\partial y_l''} \frac{\partial v_l}{\partial y_k''}}$$
$$+ \overline{\frac{\partial^2 v_i v_j}{\partial y_i' \partial y_j'} \frac{\partial^2 v_k v_l}{\partial y_l'' \partial y_k''}} - \overline{\frac{\partial^2 v_i v_j}{\partial y_i' \partial y_j'} \frac{\partial^2 v_k v_l}{\partial y_k'' \partial y_l''}}, \qquad (20)$$

a quantity which is beyond assessment. On the other hand it has been suggested that the first term of expression (20) for the source, the only one involving only second-order correlations, is in fact the dominant term. For a two-dimensional turbulent boundary layer this term very nearly reduces to

$$4 \frac{\partial U_1}{\partial y_2'} \frac{\partial U_1}{\partial y_2''} \overline{\frac{\partial v_2}{\partial y_1'} \frac{\partial v_2}{\partial y_1''}}.$$

The dominance of this term has been expected physically because the mean velocity gradient $\partial U_1/\partial y_2$ is known to be a large quantity in the inner part of the boundary layer or more precisely because the product $(\partial U_1/\partial y_2)^2 \, \overline{(\partial v_2/\partial y_1)^2}$ has a maximum value which exceeds that of any other of the fourth-order terms in expression (20). The relative importance of this mean-shear-turbulence interaction term and of all others has been discussed more formally by Kraichnan (1956) and by Hodgson (1962). But the comparison is not decisive primarily because the models of the velocity field used for such an estimate are necessarily very coarse (see, e.g., Corcos 1962). On the other hand the recent and detailed measurements of Wooldridge & Willmarth (1962) may be used to satisfy our curiosity on this point and render unnecessary estimates based upon models.

These measurements give us for a large carefully developed turbulent boundary layer, the pressure intensity at the wall, its frequency spectral density, the space-time correlation of the pressure at the wall and the space-time correlation of the pressure at a fixed point of the wall with all three components of the velocity fluctuation vector over a grid of values of the location of the velocity measuring probe. In particular, the correlation function

$$\overline{p(\mathbf{x}, t) \, \partial v_2 (\mathbf{x} + \mathbf{\xi}, t + \tau)/\partial x_1}$$

was recorded for a very complete set of values of $\mathbf{\xi}$ and τ with $x_2 = 0$. Here $\mathbf{\xi}$ is the position vector of the hot-wire probe with respect to the pressure transducer location. From these measurements one can compute directly and without
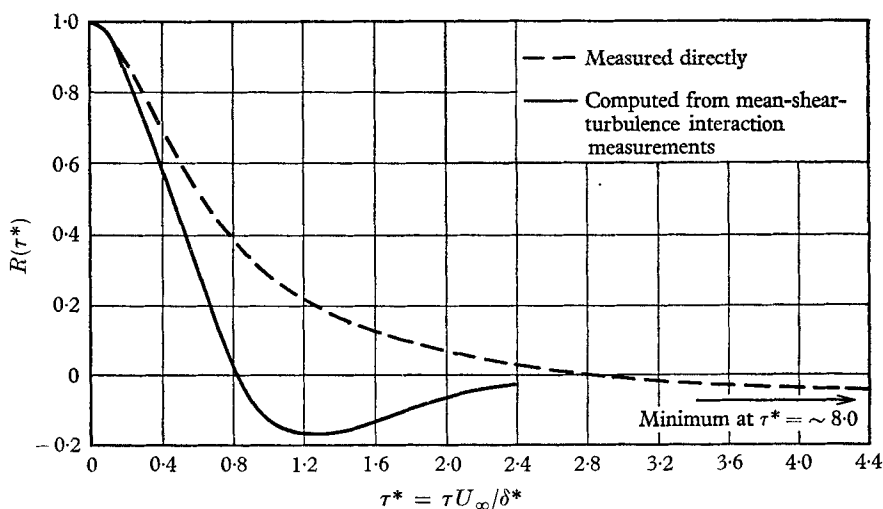

FIGURE 15. The normalized pressure covariance in a boundary-layer.
Data from Wooldridge & Willmarth.

additional assumptions, (a) the fraction of the pressure intensity at the wall contributed by the mean shear-turbulence interaction term; (b) the space and the time covariances of this contribution and (c) its average convection velocity. The method of computation is given in an appendix together with a discussion of the reliability of the results. These results are as follows.

In the boundary layer of Wooldridge & Willmarth, the linearizing assumption

$$\nabla^2 p = - 2\rho_0 \frac{\partial U_1}{\partial x_2} \frac{\partial v_2}{\partial x_1}$$

leads to an auto-correlation of the pressure at the wall, the characteristic time of which is much shorter than that of the observed pressure auto-correlation. As is shown on figure (15), the computed auto-correlation crosses the time axis for $\tau U_\infty/\delta^* = 0.82$ and is negligible beyond $\tau U_\infty/\delta^* = 2.5$, while the auto-correlation measured by Willmarth & Wooldridge (1962) crosses the time axis for $\tau U_\infty/\delta^* = 2.8$ and does not reach a maximum negative value until $\tau U_\infty/\delta^* = 8.0$. The same linearizing assumption leads to a mean-square pressure intensity at the

wall which is approximately 32 % of the observed value. The inference that the non-linear terms contribute the balance is not rigorous because as expression (20) shows, there are in fact three types of sources—originating from the product of linear terms with themselves, of linear with quadratic terms, and of quadratic terms with themselves. The computation evaluates the sum of the purely linear contributions and half the cross-contributions. However, the latter are likely to be small because they are the result of third-order correlations between typically distant points.
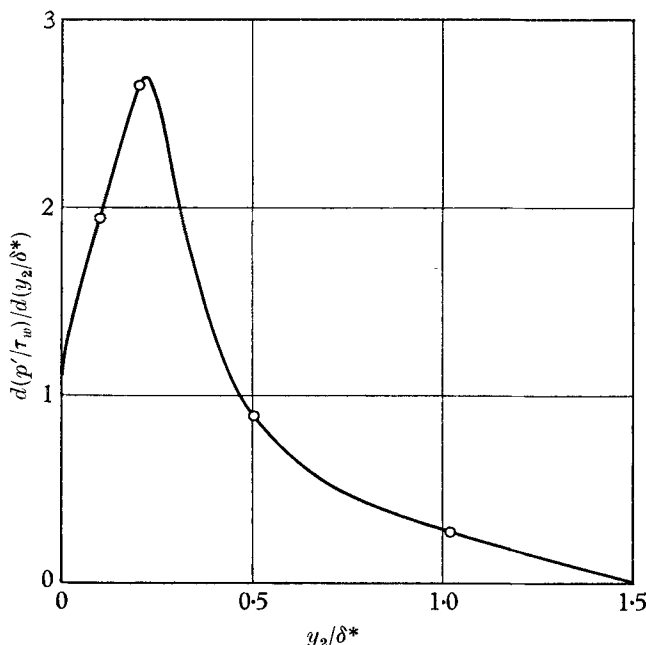

FIGURE 16. The contribution of mean shear-turbulence interaction to the pressure at the wall. $\dfrac{p'_L}{\tau_w} = 1\cdot23$; $\dfrac{p'^2_L}{p'^2} = 0\cdot314$.

The translation velocity of the linear contribution to the pressure field averages $0\cdot66U_\infty$ and increases little with separation distance. By contrast the translation velocity of the observed pressure averages $0\cdot82U_\infty$.

Figure 16 indicates what part of the boundary layer contributes linearly to the pressure at the wall by giving the result of a partial integration of the data along planes parallel to the wall. p'/τ_w is the area under the curve. Figure 17 alike shows the linear contribution of four slices of the boundary layer to the auto-correlation of the pressure at the wall. One observes that while the time and length scales of the linear pressure sources increase with y_2 and approach those of the observed wall pressure for $y_2/\delta^* = 2\cdot0$, the strength of these sources at such distances is so small as to be negligible. Thus the linear sources contribute to the wall pressure intensity and to its auto-correlation only within a narrow region, $y_2/\delta^* < 1\cdot0$ and the bulk of this contribution is found around

$$y_2/\delta^* = 0\cdot2 \quad (y^* = 440).$$

Lilley (1963) used the assumption that the linear source terms are dominant and a model of the velocity field to compute the covariance of the pressure at the wall. His results are suggestive of the observed values. But the same model also yields pressure-velocity covariances which are so different from those directly observed that the statistical description of the velocity field v_2 by the model cannot be satisfactory, and final agreement of some of the features of the computed and observed pressure fields must be regarded as fortuitous.

In summary, the velocity-pressure covariance measurements of Wooldridge & Willmarth show that for the purpose of computing turbulent pressures from given turbulent velocities, one is not justified (in an incompressible boundary layer) in linearizing the unsteady equations of motion around a known mean
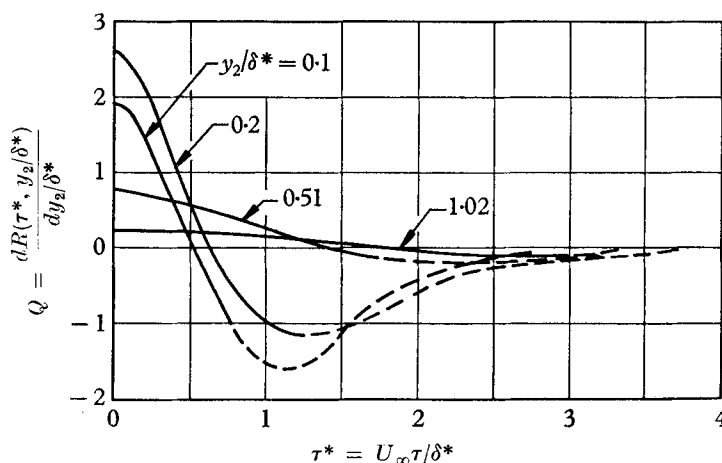

FIGURE 17. The contribution of the mean shear-turbulence interaction to the pressure at the wall: the autocorrelation contributed by various laminae of the boundary layer

$$R(\tau^*) = \int_0^\infty (Q)_{\tau^*} dy_2/\delta^*.$$

velocity. The source term obtained in this way, while significant, is not the primary cause of the low frequency, large-scale part of the observed pressures, and it is at most of the same order of importance as the non-linear source terms.

The pressure near the wall

We have just seen that the linear source terms located in the region $yu^*/\nu \leqslant 100$ do not contribute much to the pressure field (except perhaps at very high frequencies). It is very likely that the non-linear source terms are weak there also, first because the bulk of the pressure field is translated at a speed $\simeq 0.82 U_\infty$ which suggests that the average location of the pressure sources is $y^* = 3000$, and second because unless the longitudinal space scale of the non-linear source terms is, in that region, several times as large as that of the linear term, their contribution to the wall pressure would also be concentrated within an unrealistically high-frequency band. This suggests that within the narrow but interesting

region $yu^*/\nu \leqslant 100$ it is possible to express the pressure field in terms of its wall value. If we define a random pressure component (a generalized function) π by

$$\pi(x_2, \mathbf{k}, t) = \frac{1}{4\pi^2} \int_{-\infty}^{\infty} \int_{-\infty}^{\infty} p(\mathbf{x}, t) \exp \langle -i(k_1 x_1 + k_3 x_3) \rangle \, dx_1 dx_3,$$

and a source function T by

$$T(x_2, \mathbf{k}, t) = -\frac{1}{4\pi^2} \int_{-\infty}^{\infty} \int_{-\infty}^{\infty} X(x, t) \exp \langle -i(k_1 x_1 + k_3 x_3) \rangle \, dx_1 dx_3,$$

where $\mathbf{k} = (k_1, k_3)$ and if $k = |\mathbf{k}|$ then (cf. Kraichnan 1956) one may deduce from equation (3) a simple ordinary differential equation relating π and T. If one makes use of the boundary condition $(\partial p/\partial x_2)_{x_2=0} = 0$, which implies $(d\pi/dx_2)_0 = 0$, one may give the solution for π as

$$\pi(x_2, \mathbf{k}) = \pi(0, \mathbf{k}) \cosh kx_2 - \frac{1}{k} \int_0^{x_2} \sinh k(x_2 - x_2') \, T(x_2', \mathbf{k}) \, dx_2'.$$

This form of the solution emphasizes the fact that only sources found between the boundary and the field point x_2 prevent the value of $\pi(x_2, \mathbf{k})$ from being specified in terms of $\pi(0, \mathbf{k})$. The wave-number spectrum is related to $\pi(x_2, \mathbf{k})$ by

$$E(x_2, \mathbf{k}) = \frac{\langle \pi(x_2, \mathbf{k}') \, \pi(x_2, \mathbf{k}) \rangle}{\delta(\mathbf{k} + \mathbf{k}')}$$

and is therefore

$$E(x_2, \mathbf{k}) = E(0, \mathbf{k}) \cosh^2 kx_2 - \frac{2 \cosh kx_2}{k' \delta(\mathbf{k} + \mathbf{k}')} \int_0^{x_2} \sinh k(x_2 - x_2') \, \overline{T(x_2', \mathbf{k}) \, \pi(0, \mathbf{k}')} \, dx_2'$$

$$+ \frac{1}{kk'} \frac{1}{\delta(\mathbf{k} + \mathbf{k}')} \int_0^{x_2} \int_0^{x_2} \sinh k(x_2 - x_2') \sinh k(x_2 - x_2'') \, \overline{T(x_2', \mathbf{k}) \, T(x_2'', \mathbf{k}')} \, dx_2' dx_2''.$$
$$\tag{21}$$

Now let us choose x_2 small enough so that $x_2 u^*/\nu \leqslant 100$. For the conditions of Wooldridge & Willmarth's experiment, this corresponds to $x_2/\delta^* \leqslant 0\cdot055$ and for such distances from the wall, (a) $kx_2 \ll 1$ for the bulk of the energy spectrum (which is found for $k\delta^* < 5$), (b) the integral of the covariances of the pressure sources over the lamina $0 \leqslant x_2' \leqslant x_2$ yields a negligible contribution to the pressure at the wall. Under the same conditions it is easy to show that the second integral on the right-hand side of (21) is of order at most (kx_2) times the first and that the latter is not only small with respect to $E(0, k)$ but also small with respect to $(kx_2)^2 \, E(0, \mathbf{k})$, so that

$$E(x_2, \mathbf{k}) \simeq E(0, \mathbf{k}) \cosh^2 kx_2 \tag{22}$$

except for very high wave-numbers. An expression for $\overline{p^2}(x_2)$ can easily be deduced from (22).

Equation (22) is the solution which would correspond to the equation and boundary conditions

$$\nabla^2 p = 0; \quad \begin{cases} d\pi/dx_2 = 0 \quad \text{at} \quad x_2 = 0, \\ \pi(x_2, \mathbf{k}) \text{ given at } x_2 = \text{some specified distance, } h, \text{ from the wall.} \end{cases}$$

It follows that, while the momentum flux fluctuations are very large within this region, they do not affect directly the pressure fluctuations locally, essentially

because they are spatially too incoherent over neighbourhoods within which momentum flux fluctuations originating further from the wall give rise to strongly correlated pressure fluctuations.

Appendix. The computation of the covariance of the pressure from the linear source term

The computation uses the measurements of Wooldridge & Willmarth (1962) of mean velocity, U_1, intensity of the time derivative of the velocity component normal to the wall $\dot{v}$ (for simplicity we redefine here v_2 as v) and covariance of p at the wall with $\dot{v}$.

From equation (6) which assumes $(\partial p/\partial x_2)_{x_2=0} = 0$ and the assumption that only the first term on the right of equation (3) (the 'linear' term) contributes appreciably to the pressure, we get for a point $\mathbf{x} = (x_1, 0, x_3)$ on the wall

$$p(x_1, 0, x_3, t) = \frac{\rho_0}{\pi} \int_{y_2 \geqslant 0} \frac{\partial U_1}{\partial y_2} \frac{\partial v}{\partial y_1} \frac{d\sigma(\mathbf{y})}{|\mathbf{y} - \mathbf{x}|},$$

and hence

$$\overline{p(\mathbf{x}, t) \frac{\partial v}{\partial y_1'}} (\boldsymbol{\zeta}, t') = C(\boldsymbol{\zeta}, \tau) = \frac{\rho_0}{\pi} \int_{y_2 \geqslant 0} \frac{\partial U_1}{\partial y_2} \overline{\frac{\partial v}{\partial y_1} \frac{\partial v}{\partial y_1'}} \frac{d\sigma(y)}{|\mathbf{y} - \mathbf{x}|}.$$

Here $\qquad \boldsymbol{\zeta} = \mathbf{y}' - \mathbf{x}, \quad \tau = (t' - t); \quad \overline{\frac{\partial v}{\partial y_1} \frac{\partial v}{\partial y_1'}} = f(\mathbf{y}', \mathbf{y} - \mathbf{y}', \tau).$

On the other hand

$$R(\boldsymbol{\xi}, \tau) = \overline{p(\mathbf{x}, t)\, p(\mathbf{x} + \boldsymbol{\xi}, t + \tau)}$$

$$= \frac{\rho_0^2}{\pi^2} \int_{y_2 \geqslant 0} \int_{y_2' \geqslant 0} \frac{\partial U_1}{\partial y_2} \frac{\partial U_1}{\partial y_2'} \overline{\frac{\partial v}{\partial y_1} \frac{\partial v}{\partial y_1'}} \frac{d\sigma(\mathbf{y})\, d\sigma(\mathbf{y}')}{|\mathbf{y} - \mathbf{x}|\, |\mathbf{y}' - \mathbf{x}'|},$$

where $x' = \mathbf{x} + \boldsymbol{\xi}$, is another point on the wall. Hence

$$R(\boldsymbol{\xi}, \tau) = \frac{\rho_0}{\pi} \int_{y_2' \geqslant 0} \frac{\partial U_1}{\partial y_2'} \frac{C(\boldsymbol{\zeta}, \tau)}{|\mathbf{y}' - \mathbf{x}'|} d\sigma(\mathbf{y}'),$$

and in particular

$$\overline{p^2}(\mathbf{x})_{x_2=0} = \frac{\rho_0}{\pi} \int_{y_2' > 0} \frac{\partial U_1}{\partial y_2'} \frac{C(\boldsymbol{\zeta}, 0)}{|\mathbf{y}' - \mathbf{x}|} d\sigma(\mathbf{y}'), \qquad (a)$$

$$R(0, \tau) = \frac{\rho_0}{\pi} \int_{y_2' > 0} \frac{\partial U_1}{\partial y_2'} \frac{C(\boldsymbol{\zeta}, \tau)}{|\mathbf{y}' - \mathbf{x}|} d\sigma(\mathbf{y}'). \qquad (b)$$

Now Wooldridge & Willmarth have measured a function $R_{p\dot{v}}$ which is easily related to C. For data for

$$R_{p\dot{v}} = \frac{\overline{p(\mathbf{x}, t)\, \dot{v}(x + \zeta, t + \tau)}}{(\overline{p^2}\, \overline{\dot{v}^2})^{\frac{1}{2}}}$$

shows that for sufficiently short times and to a very good accuracy

$$R_{p\dot{v}}(0, \zeta_2, 0, \tau) = R_{p\dot{v}}\{\zeta_1, \zeta_2, 0, \tau + (\zeta_1/U_1)\},$$

where U_1 is the mean velocity at ζ_2. This means that delay time and longitudinal separations can be interchanged for sufficiently small delay times, so that

$$R_{pv}(\zeta, \tau) = -\frac{\overline{p(x,t)\, \partial v\, (x+\zeta, t+\tau)/\partial y_1}}{[\overline{p^2\, (\partial v/\partial y_1')^2}]^{\frac{1}{2}}} = \frac{C(\zeta, \tau)}{[\overline{p^2\, (\partial v/\partial y_1')^2}]^{\frac{1}{2}}} = c(\zeta, \tau),$$

and that

$$C(\zeta_1, \zeta_2, \zeta_3, \tau) = C\{0, \zeta_2, \zeta_3, \tau - (\zeta_1/U_1)\}.$$

The delay times τ for which these relations are valid vary with ζ_2 as shown in the following table

ζ_2/δ^*	0·1	0·2	0·5	1·0	2·0
$\tau U_\infty/\delta^* \leqslant$	0·9	1·3	1·8	2·7	5·0

For larger delay times, account could be taken of the progressive decrease of the source strength, but this is not necessary for the computations presented, since the character of the computed auto-correlation of p at the wall is apparent for $\tau U_\infty/\delta^* < 0\cdot8$. Thus the measurements of $R_{pv}\{0, \zeta_2, \zeta_1, \tau - (\zeta_1/U_1)\}$ supply the integrand in equations such as (a) and (b). The integration is carried out numerically over planes parallel to the wall first, after contours of $C(\zeta, \tau)_{\zeta_2}$ have been plotted and by using a fine grid. Finally, the integration is performed in the y_2' direction normal to the wall after drawing smooth curves through the points obtained from the partial integration. The auto-correlation of the observed pressure (figure 15) was measured by Willmarth & Wooldridge (1962).

Accuracy

The data provide several hundred values of R_{pv} for well-chosen values of ζ and τ. In addition Wooldridge & Willmarth have measured R_{pv} independently and this provides both a consistency check and a means of assessing with some precision the asymptotic values of R_{pv}, because, over the significant region of integration, whenever R_{pv} becomes too small to be assessed with accuracy $[R_{pv}(\tau)]_\zeta$ has a well-defined (though small) slope. It is found that the effect of these asymptotic tails of R_{pv} are negligible.

The accuracy of the inferences made makes variable demands on the accuracy of the data. For instance, the probable error in the computation of the mean-square intensity is estimated as 20–30 %, but the probable error in the delay time for the first zero of the auto-correlation curve is not likely to exceed 10 % even if one allows for very large systematic errors in the data (for which there seems to be no evidence if we except the finite space resolution of the pressure transducer used).

REFERENCES

BAKEWELL, H. P., CAREY, G. F., LIBUKA, J. J., SCHLOEMER, H. H. & VON WINKLE, W. A. 1962 Wall pressure correlations in turbulent pipe flow. *U.S. Navy Under-water Sound Laboratory Report* no. 559.

BULL, M. K. 1963 Properties of the fluctuating wall-pressure field of a turbulent boundary layer. *University of Southampton, A.A.S.U. Report*, no. 234.

BULL, M. K. & WILLIS, J. L. 1961 Some results of experimental investigations of the surface pressure field due to a turbulent boundary layer. *University of Southampton, A.A.S.U. Report*, no. 199.

CORCOS, G. M. 1962 Pressure fluctuations in shear flows. *University of California Inst. of Eng. Res. Report, Series* 183, no. 2.

CORCOS, G. M. 1963 On the resolution of pressure in turbulence. *J. Acoust. Soc. Amer.* **35**, no. 2.

FAVRE, A. J., GAVIGLIO, J. J. & DUMAS, R. 1957 Space-time double correlations in a turbulent boundary layer. *J. Fluid. Mech.* **3**, 313.

HARRISON, M. 1958 Pressure fluctuations on the wall adjacent to a turbulent boundary layer. *David Taylor Model Basin Report*, no. 1260.

HODGSON, T. H. 1962 Pressure fluctuations in shear flow turbulence. *College of Aeronautics, Cranfield, Note*, no. 129.

KISTLER, A. L. & CHEN, W. S. 1962 The fluctuating pressure field in a supersonic turbulent boundary layer. *Jet Propulsion Laboratory Tech. Rep.*, no. 32–277.

KLEBANOFF, P. S. 1954 Characteristics of turbulence in a boundary layer with zero pressure gradient. *Nat. Adv. Comm. Aero. (Wash.) Tech. Note*, no. 3178.

KRAICHNAN, R. H. 1956 Pressure fluctuations in turbulent flow over a flat plate. *J. Acoust. Soc. Amer.* **28**, 378.

LILLEY, G. M. 1963 Wall pressure fluctuations under turbulent boundary layers at subsonic and supersonic speeds. *College of Aeronautics, Cranfield, COA Note* 140.

LILLEY, G. M. & HODGSON, T. H. 1960 On surface pressure fluctuations in turbulent boundary layers. *AGARD Report*, no. 276.

PHILLIPS, O. M. 1954 Surface noise from a plane turbulent boundary layer. *Aero. Res. Counc. (London)*, no. 16,963.

RICHARDS, E. J. 1961 Aerodynamic noise sources. *Paper B. 3, 'Control of Noise' conference, National Physical Laboratory, Teddington.*

SERAFINI, J. S. 1962 Wall pressure fluctuations in a turbulent boundary layer. *Ph.D. Thesis, Case Institute of Technology.*

SKUDRZYK, E. F. & HADDLE, C. P. 1960 Noise production in a turbulent boundary layer by smooth and rough surfaces. *J. Acoust. Soc. Amer.* **32**, 19.

TOWNSEND, A. A. 1956 *The structure of turbulent shear flow.* Cambridge University Press.

UBEROI, M. A. & KOVASNAY, L. S. G. 1953 On the mapping of random fields. *Quart. Appl. Math.* **10**, 375.

VON WINKLE, A. A. 1960 Some measurements of longitudinal space-time correlations of wall pressure fluctuations in turbulent pipe flow. *Univ. of California Inst. of Eng. Res. Report, Series* 82, Issue no. 20.

WILLMARTH, W. W. 1957 Space-time correlations and spectra of wall-pressure in a turbulent boundary layer. *Nat. Adv. Comm. Aero. Tech. Mem.* no. 3-17-59 W.

WILLMARTH, W. W. & WOOLDRIDGE, C. E. 1962 Measurements of the fluctuating pressure at the wall beneath a thick turbulent boundary layer. *J. Fluid Mech.* **14**, 187.

WOOLDRIDGE, C. E. & WILLMARTH, W. W. 1962 Measurements of the correlation between the fluctuating velocities and fluctuating wall pressures in a thick turbulent boundary layer. *Univ. of Michigan, ORA Report* no. 0-2920-2-T.